GEOPHYSICAL TRANSACTIONS 1985
Vol. 31. No. 4. pp. 339–357

FAST EVALUATION OF RADIAL AND VERTICAL MAGNETIC FIELDS NEAR A RECTANGULAR LOOP SOURCE ON A LAYERED EARTH

Walter L. ANDERSON*

A fast Hankel transform (FHT) algorithm is used to compute simultaneously parametric (or geometric) soundings for radial and vertical magnetic fields inside or outside a rectangular loop source on the surface of a layered earth. The FHT uses concepts of related and lagged convolutions (linear digital filtering), and, when applied to the rectangular loop problem, reduces each field calculation to four elementary spline integrations. For parametric soundings, the FHT is called once for each frequency; for geometric soundings, only a single execution of the FHT is required to obtain both field components. Numerical comparisons of the FHT method with existing dipole, circular, and other rectangular loop forward solutions show that at least three-figure accuracy is achieved with greatly reduced computation time. Consequently, future inverse solutions in both frequency- and time-domains would become as practical for a rectangular loop as for a dipole source.

Keywords: electromagnetic methods, numerical modeling, frequency domain, layered model, Hankel transform

1. Introduction

Well known methods exist for calculating the electromagnetic (EM) fields at any distance from an oscillating vertical magnetic dipole or horizontal dipole source [e.g., FRISCHKNECHT 1967; WAIT 1958; WAIT 1966]. Linear digital filtering algorithms [e.g., ANDERSON 1979] provide rapid and accurate calculations for dipole sources. KAUAHIKAUA [1978] presented a method for computing the electric and magnetic field components about a straight horizontal finite-length grounded wire source over a layered earth. Recently, PODDAR [1983] developed the solution for the vertical magnetic field about a rectangular loop source of current on a multilayered earth. Poddar's solution used four separate double numerical integrations, and by superposition, obtained the total magnetic field inside or outside the rectangular loop at arbitrary positions. KRISTENSSON [1983] also presented a method of computing the EM field components in a layered earth for a general current distribution, including a horizontal rectangular loop source; his method, however, required direct evaluation of integrals and series involving Bessel functions.

The question of why a rectangular loop is specified here over a more general or arbitrary line segment loop naturally arises. BOERNER and WEST [1984]

* U.S. Geological Survey, Box 25046 M. S. 964, Denver Federal Center, Denver, Colorado 80225
Manuscript received: 10 June, 1985

presented an interesting method to compute efficiently the EM fields of an extended wire source. They suggested using the FHT algorithm (as proposed in the present paper, and published by ANDERSON, [1982]) to compute all Hankel transforms for a given field component by lagged convolution, and as required over all spatial distances for a given wire configuration. The total field is then computed by a weighted summation using weights derived from a precomputed quintic spline. However, the technique is often applied in practice to simple geometric sources that are easy to set up, such as a square or rectangular loop. This simplifies recording end-point coordinates in the measurement environment. Boerner and West's method is quite similar to my method, except they apparently proposed using it to compute only a single field component for each FHT execution.

This paper presents a new method to compute in one pass the radial (H_r) and vertical (H_z) magnetic fields about a rectangular loop source on a layered earth. The basic formulations for each field component reduce to four adaptive finite spline integrations, after first computing all related and lagged Hankel transforms using a single call to the FHT algorithm. Parametric (frequency) or geometric (distance) soundings for H_r and H_z can be computed at arbitrary points inside or outside the rectangular loop source of finite dimensions. The rectangular loop is assumed to be placed on the earth's surface and the layers are parallel to the surface. Displacement currents are neglected (quasi-static case) for all computations.

Recent advances in evaluating Hankel transforms by the FHT algorithm [ANDERSON 1982] lead naturally to this new approach, which extends PODDAR'S [1983] solution for H_z to include H_r (or simultaneously H_x and H_y) field components. This method is intended to provide a practical tool for studying the frequency response near the loop where a dipole source cannot be assumed. In most physical situations, it is easier to lay out a square or rectangular wire loop than a circular loop; consequently, this method should be more appropriate (and efficient) than an exclusively circular loop computation [e.g., RYU et al. 1970].

Some tests were made with small loop sizes and large spacings to simulate a dipole-dipole case. Both H_r and H_z results agreed to about 3-place accuracy with existing dipole source results [FRISCHKNECHT 1967]. Tests were also made using the same rectangular loop source and models as given by PODDAR [1983], which included H_r as well as H_z components; these results are discussed and illustrated in a following section.

A natural extension of the rectangular loop frequency-domain response to the time-domain can be made using a suitable Fourier transformation; e.g., see ANDERSON [1985], where only the H_z transient response is treated.

2. Theory and computations

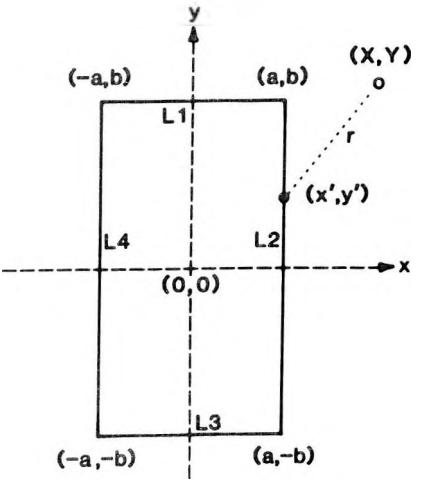

Fig. 1. Loop geometry at $z=0$ (earth's surface), where (X, Y) is the observation point, and (x', y') is any point on the rectangular loop source

1. ábra. A hurok geometriája $z=0$-nál (a föld felszínén), ahol (X, Y) a mérési pont és (x', y') a téglalap alakú hurokforrás tetszőleges pontja

Рис. 1. Геометрические данные контура. $z=0$ (поверхность земли), (X, Y) – точка измерения, (x', y') – любая точка прямоуголного контура

Figure 1 shows the coordinate system and geometry of a rectangular loop. Line segments $[(-a, b); (a, b)]$, $[(a, -b); (a, b)]$, $[(-a, -b); (a, -b)]$, and $[(-a, -b); (-a, b)]$ are denoted respectively as lines *L1*, *L2*, *L3*, and *L4*. The length of lines *L1* and *L3* is *2a*, and of lines *L2* and *L4* is *2b*.

The magnetic field inside or outside a rectangular loop can be formally obtained by a suitable summation of the results from four separate finite grounded wires as defined in KAUAHIKAUA [1978]. However, the rectangular loop problem is simpler, because there are no currents injected into the earth at the ends of each wire segment. The formulas in KAUAHIKAUA [1978] are written in a form such that the contribution from currents at the wire ends may be readily neglected; this fact will be used below in the H_r loop development. PODDAR [1983] derived his solution for a rectangular loop by starting with the electric field due to a magnetic dipole and then applying reciprocity. From PODDAR [1983], the vertical magnetic field H_z at any point (X, Y) for a loop source with current $I \exp(i\omega t)$ is

$$H_z = I(H_{L1} + H_{L2} + H_{L3} + H_{L4})/2\pi, \tag{1}$$

where

$$\begin{aligned}
H_{L1} &= -(b-Y) \int_{-a}^{a} (\mathrm{d}x'/r) \int_{0}^{\infty} k(\lambda)\, \mathrm{J}_1(\lambda \mathrm{r})\, \mathrm{d}\lambda, \qquad \mathrm{r}^2 = \mathrm{R}_1^2 \\
H_{L2} &= -(a-X) \int_{-b}^{b} (\mathrm{d}y'/r) \int_{0}^{\infty} k(\lambda)\, \mathrm{J}_1(\lambda \mathrm{r})\, \mathrm{d}\lambda, \qquad \mathrm{r}^2 = \mathrm{R}_2^2 \\
H_{L3} &= -(b+Y) \int_{-a}^{a} (\mathrm{d}x'/r) \int_{0}^{\infty} k(\lambda)\, \mathrm{J}_1(\lambda \mathrm{r})\, \mathrm{d}\lambda, \qquad \mathrm{r}^2 = \mathrm{R}_3^2 \\
H_{L4} &= -(a+X) \int_{-b}^{b} (\mathrm{d}y'/r) \int_{0}^{\infty} k(\lambda)\, \mathrm{J}_1(\lambda \mathrm{r})\, \mathrm{d}\lambda, \qquad \mathrm{r}^2 = \mathrm{R}_4^2
\end{aligned} \tag{2}$$

$$\begin{aligned} R_1^2 &= (x'-X)^2+(b-Y)^2, \\ R_2^2 &= (a-X)^2+(y'-Y)^2, \\ R_3^2 &= (x'-X)^2+(b+Y)^2, \\ R_4^2 &= (a+X)^2+(y'-Y)^2, \end{aligned} \tag{3}$$

and $k(\lambda)$ is a recursive complex kernel function [PODDAR 1983] containing the factor $\exp(-\lambda z)$, $z>0$. The Hankel transforms in equations (2) do not converge if the observation point is on the surface ($z=0$). To overcome this problem, Poddar set $z = 10^{-3}$ meters in $k(\lambda, z)$. This approach was not used in this paper, because some advantage is gained using $z=0$ and the fast converging formulas derived by KAUAHIKAUA [1978]. Here the half-space response was removed from $k(\lambda)$ and a closed-form expression added outside the integrals. This modification to equations (2) becomes

$$\begin{aligned} H_{L1} &= -(b-Y)\int_{-a}^{a} (\mathrm{d}x'/r)\{h_z^S(r)\}, \quad r^2 = R_1^2 \text{ in (3)} \\ H_{L2} &= -(a-X)\int_{-b}^{b} (\mathrm{d}y'/r)\{h_z^S(r)\}, \quad r^2 = R_2^2 \text{ in (3)} \\ H_{L3} &= -(b+Y)\int_{-a}^{a} (\mathrm{d}x'/r)\{h_z^S(r)\}, \quad r^2 = R_3^2 \text{ in (3)} \\ H_{L4} &= -(a+X)\int_{-b}^{b} (\mathrm{d}y'/r)\{h_z^S(r)\}, \quad r^2 = R_4^2 \text{ in (3)}, \end{aligned} \tag{4}$$

where

$$h_z^S(r) = \frac{1}{\delta}\int_0^{\infty} f_4(\lambda\delta)\, J_1(\lambda r)\,\mathrm{d}\lambda - \mathrm{i}\,\delta\,[h_z^0(B)]/(2r^4), \tag{5}$$

$$h_z^0(B) = 3-\{3+3B(1+i)+2iB^2\}\exp[-(1+i)B], \quad i=(-1)^{1/2},$$

$$B = r/\delta, \quad \delta = [2/(\sigma_1\mu_0\omega)]^{1/2}, \quad \omega = 2\pi f, \quad f>0 \text{ frequency (Hertz)},$$

$$\sigma_1 = \text{conductivity of layer 1 (Siemens/m)},$$

$$\mu_0 = 4\pi 10^{-7} \text{ permeability of free space (Weber/Am)},$$

and

$f_4(\lambda\delta)$ is defined in KAUAHIKAUA [1978] as $f_4(g)$.

(The complex recursive expressions used in $f_4(g)$ and all associated formulas and notations are explicitly listed in KAUAHIKAUA [1978, p. 1019–1021], and will not be repeated here; note that $f_4(g)$ contains all the parameters defining the layered earth model.)

Equation (5) is a continuous complex function defined for all r in $[r_{min}, r_{max}]$, where r_{min} and r_{max} are the respective minimum and maximum values of distances from (X, Y) to all points on the rectangular loop. The Hankel transform and

other expressions in equation (5) are in general required over different subintervals of r for each definite integral in equations (4). If equation (5) is sufficiently discretized over all r in $[r_{min}, r_{max}]$, then a single predetermined spline interpolating function (denoted by superscript S) can be used instead of equation (5) directly for each definite integral. Thus the four double integrations in equations (2) are essentially replaced by four single spline integrations in equations (4). The Hankel transform evaluations in equation (5), coupled with a lagged convolution (or discretation) over all r in $[r_{min}, r_{max}]$, is greatly facilitated by using the FHT algorithm, which is the principal reason for the fast computation times possible using equation (5). Once equation (5) is precomputed by lagged convolution and saved for all r in $[r_{min}, r_{max}]$, then equations (4) can be evaluated by elementary spline integration [ALBERG et al., 1967, p. 44], or by adaptive Gaussian quadrature [PATTERSON 1973] using a spline-defined integrand. Note that the above procedure must be repeated for each new frequency for parametric soundings, but only a *single* execution of the FHT is needed for geometric soundings.

The H_r radial field component is derived by analogy with H_z above, using the formula for $H_y^{f_{in}}$ in KAUAHIKAUA [1978], but neglecting the term due to the wire ends. The H_r field at any point (X, Y) becomes,

$$H_r = H_x(X/R_0) + H_y(Y/R_0), \qquad R_0^2 = X^2 + Y^2, \tag{6}$$

where

$$\begin{aligned}
H_x &= I(-h_{L2} + h_{L4})/2\pi, & H_y &= I(-h_{L1} + h_{L3})/2\pi,\\
h_{L1} &= -\int_{-a}^{a} (\mathrm{d}x'/r)\{h_r^S(r)\}, & r^2 &= R_1^2 \text{ in (3)}\\
h_{L2} &= -\int_{-b}^{b} (\mathrm{d}y'/r)\{h_r^S(r)\}, & r^2 &= R_2^2 \text{ in (3)}\\
h_{L3} &= -\int_{-a}^{a} (\mathrm{d}x'/r)\{h_r^S(r)\}, & r^2 &= R_3^2 \text{ in (3)}\\
h_{L4} &= -\int_{-b}^{b} (\mathrm{d}y'/r)\{h_r^S(r)\}, & r^2 &= R_4^2 \text{ in (3)},
\end{aligned} \tag{7}$$

$$\begin{aligned}
h_r^S(r) = -\{B\int_0^\infty f_4(\lambda\delta)\,J_0(\lambda r)\,\mathrm{d}\lambda + \frac{1}{r}[\beta(I_0(\beta)K_1(\beta) -\\
- I_1(\beta)K_0(\beta)) - 2I_1(\beta)K_1(\beta)]\},
\end{aligned} \tag{8}$$

$$\beta = B(1+i)/2, \qquad i = (-1)^{1/2},\ B = r/\delta,$$

and I_0, I_1, K_0, K_1 are modified Bessel functions of orders 0 and 1.

Equation (8) is replaced by a precomputed spline function analogous to equation (5). Modified Bessel functions are needed initially in equation (8) to compute the spline coefficients, but they are not required while performing the four spline integrations in equations (7).

Computation of all H_z and H_r Hankel transforms required in equations (5) and (8) are obtained rapidly by the FHT algorithm using related and lagged convolutions [ANDERSON 1982]. Observe that both Hankel transforms in equations (5) and (8) have the same kernel function $f_4(\lambda\delta)$, but have different order Bessel functions. The FHT algorithm was developed to integrate in parallel both orders 0 and 1 for any arbitrary transform argument range by lagged convolution, and to simultaneously provide for algebraically related kernels (in this case, the kernels are identical). Thus, with *one* execution of the FHT algorithm, a complete 2-column matrix of Hankel transforms (orders 0 and 1) is computed over a small digitized interval in r equivalent to the digital filter sampling interval (specifically, 0.2 in log-space). Therefore, both H_r and H_z field components are obtained in nearly the same time as would be required to evaluate a single component. Optionally, the H_x and H_y orthogonal components at (X, Y) can be computed instead of H_r. Observe from equation (6) that $H_r = H_x$ if $Y=0$, and $H_r = H_y$ if $X=0$.

The Hankel transforms in equations (5) and (8) are zero for a half-space model, which is one benefit of using the $z=0$ formulas from KAUAHIKAUA [1978], instead of the $z>0$ case of PODDAR [1983]. The general expressions in equations (5) and (8) apply to either parametric or geometric soundings, thus providing a unified mathematical treatment.

3. Computer program

A computer program (HRZRECT) that implements the algorithm presented in this paper is documented in ANDERSON [1984]. The code was written in FORTRAN–77 for a VAX–11/780 VMS system, and is listed in ANDERSON [1984].

4. Examples and discussion

Examples of soundings for various models computed using program HRZRECT are summarized graphically in this section. Numerical results and VAX execution times corresponding to these plots are tabulated in ANDERSON [1984]. Typically, complete geometric soundings for both H_r and H_z take about 2 to 5 CPU-seconds on the VAX computer. As would be expected, execution times are slightly larger for points very near the source. In general, it is recommended that (X, Y) should be chosen such that $r > \min(a, b)/10$ for all r. Usually, points very close to the source loop are of little practical interest, and should be avoided. Furthermore, a small saving is achieved in summing equations (1) and (6) whenever (X, Y) is chosen symmetrical with respect to the loop sides (e.g., $X>0$, $Y=0$).

The H_z results plotted in Figures 2 and 3 duplicate respectively the parametric and geometric soundings illustrated in PODDAR [1983]. The same models were used to compute H_r in parallel with H_z, and are also plotted in Figures 2 and 3.

PODDAR [1983] compared his results with RYU et al. [1970], where the latter authors used a circular loop source. As shown in *Figure 2*, the FHT method agrees quite well with the results from PODDAR [1983, Fig. 2] and RYU et al. [1970]. The amplitude scale in Figure 2 is unnormalized (Amps/m.) as in Poddar's Figure 2; however, a normalized mutual coupling ratio H/Z_0 was used in *Figure 3*, instead of amplitude given in dB as in Poddar's Figure 3. The normalization factor Z_0 is defined as the free space field from a rectangular loop source of current and is given by PODDAR [1982, p. 104]. The H_z/Z_0 mutual coupling ratio amplitude in Figure 3 approaches unity for all soundings near the loop for $X \geq 200$; and as expected, the H_r/Z_0 amplitude approaches zero near the loop center for all H_r soundings.

The behavior of the H_r and H_z fields outside the rectangular loop for the same model as in Figure 3 is depicted in *Figure 4*. Figure 4 shows the normalized H_r and H_z field geometric soundings for $Y=0$ and $X \geq 300$. Note that the amplitude of H_z/Z_0 approaches unity near the source (as in Figure 3), but depending on the layer thicknesses, it can either increase or decrease from unity as X increases. The behavior of H_r/Z_0 similarly approaches zero on either side of the nearest rectangle leg. The field components are continuous as the source is approached by (X, Y), but nevertheless, they cannot be evaluated accurately at extremely small r values.

The field components in the first quadrant outside the loop, near the corner point (250, 250), are illustrated in *Figure 5*, where $Y=275$ and $X \geq 0$ were used in the geometric soundings. The flat responses for $0 \leq X < 250$ in both amplitude and phase spectra are due almost entirely to the nearest rectangular leg. For $X > 250$, all four legs begin to contribute more to the total field at larger r distances.

As a final example of parametric soundings, the model in Figure 2 was used with two different layer thicknesses, and computed at the observation point (2, 3), wich was specifically offset from (0, 0) so that H_r was non-zero. The results are given in *Figure 6*.

The unnormalized amplitude shapes for H_r and H_z in Figures 2 and 6 are somewhat similar; however, a noticeable phase jump from -180 to $+180$ degrees occurs for H_r inside but not outside the loop (compare Figures 2d and 6d). This is an artifact of representing phase angles in the range $(-180, 180)$ degrees instead of (0, 360) degrees. A choice was made so that the phase angles of H_z and H_z/Z_0 were in the same quadrants inside or outside the loop, whereas the phase angles of H_r or H_r/Z_0 differed by 180 degrees inside and outside. Thus the phase angles of the unnormalized fields and normalized fields are identical and in the same quadrants for points outside the loop, but are 180 degrees out-of-phase for points inside the loop. Regardless of how phase angles are

defined for normalized or unnormalized fields, this could lead to difficulty, for example, in joint inversion of phase data taken both inside and outside a rectangular loop. Of course, the use of real and quadrature soundings (instead of amplitude and phase) would alleviate this cumbersome situation.

Fig. 2. Parametric soundings outside a square loop ($a = b = 10$ m) at a distance of $Y = 100$ m from the loop center, and computed over a given induction number ($B = R_0/\delta$) range. The 2-layer model form PODDAR [1983, Fig. 2] was used, where $\sigma_1 = 0.01$ S/m, $\sigma_2 = 0.3$ S/m, and h was varied as indicated in the legends
a) Unnormalized amplitude H_z versus B,
b) phase H_z versus B,
c) unnormalized amplitude H_r versus B, and
d) phase H_r versus B

2. ábra. Paraméter szondázások a négyzetalakú hurkon kívül ($a = b = 10$ m), a hurok középpontjától $Y = 100$ m távolságra, egy adott indukció szám ($B = R_0/\delta$) tartományon számítva. PODDAR [1983, 2. ábra] 2-réteges modelljét használtuk, ahol $\sigma_1 = 0{,}01$ S/m, $\sigma_2 = 0{,}3$ S/m és h úgy változott, ahogy azt a jelmagyarázat feltünteti
a) A normálatlan H_z amplitúdó B függvényében,
b) a H_z fázis B függvényében,
c) a normálatlan H_r amplitúdó B függvényében és
d) a H_r fázis B függvényében

Рис. 2. Параметрические зондирования вне прямоуголного контура ($a = b = 10$ м) в расстоянии $Y = 100$ м от центра контура; для данного интервала чисел индукции ($B = R_0/\delta$). Использован двухслойный модель ПОДДАРА [1983, рис. 2], при которым: $\sigma_1 = 0{,}01$ сименс/м, $\sigma_2 = 0{,}3$ сименс/м. h изменяется согласно рисунку
а) ненормированная амплитуда H_z в зависимости от B,
b) фаза H_z в зависимости от B,
c) ненормированная амплитуда H_r в зависимости от B,
d) фаза H_r в зависимости от B

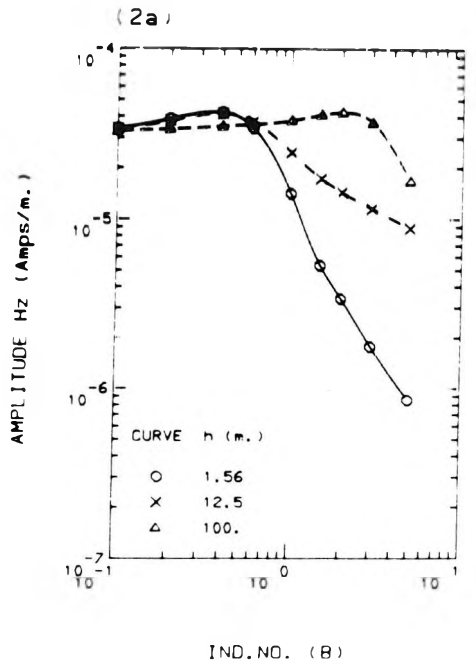
(2a)
AMPLITUDE Hz (Amps/m.)
CURVE h (m.)
1.56
12.5
100.
IND.NO. (B)

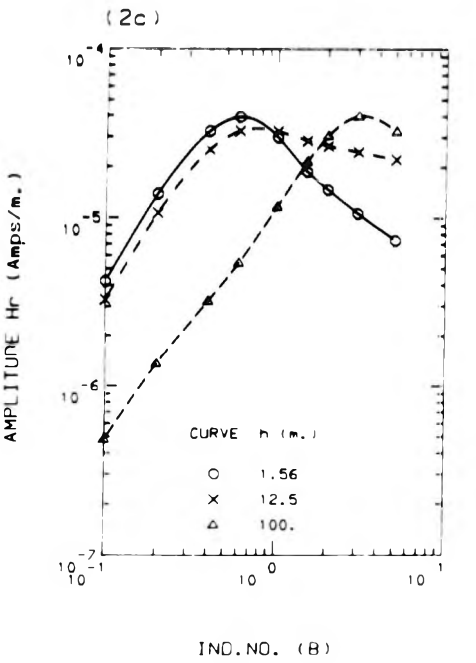
(2c)
AMPLITUDE Hr (Amps/m.)
CURVE h (m.)
1.56
12.5
100.
IND.NO. (B)

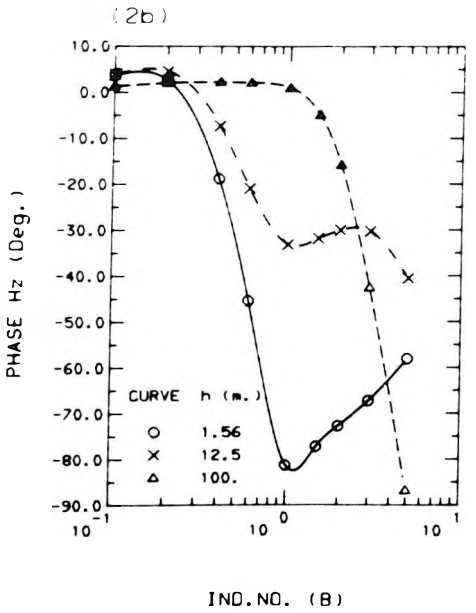
(2b)
PHASE Hz (Deg.)
CURVE h (m.)
1.56
12.5
100.
IND.NO. (B)

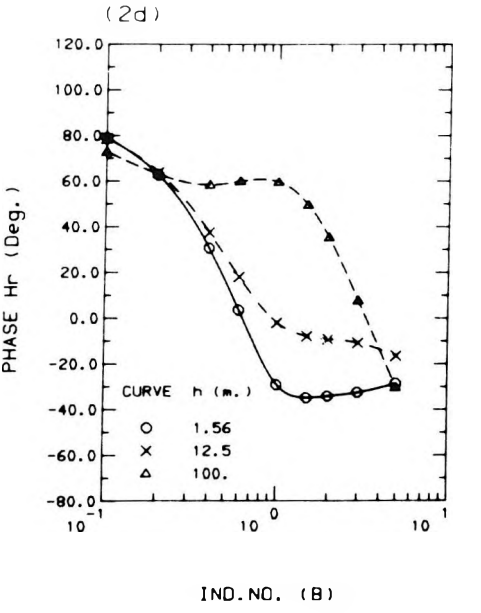
(2d)
PHASE Hr (Deg.)
CURVE h (m.)
1.56
12.5
100.
IND.NO. (B)

Fig. 3. Geometric soundings inside a square loop ($a=b=250$ m) at $Y=0$ where X was varied from 25 to 225 m in increments of 25 m. The 3-layer model from PODDAR [1983, Fig. 3] was used, where $\sigma_1=0.01$ S/m, $\sigma_2=0.03$ S/m, $\sigma_3=0.001$ S/m, $h_1=3$ m, $f=1344$ Hertz, and h_2 was varied as indicated in the legends
a) Normalized amplitude H_z/Z_0 versus X,
b) phase H_z/Z_0 versus X,
c) normalized amplitude H_r/Z_0 versus X, and
d) phase H_r/Z_0 versus X

3. ábra. Geometriai szondázás a négyzet alakú hurkon belül ($a=b=250$ m) $Y=0$-nál, X pedig 25-től 225 m-ig növekedett, 25 m-es lépésekben. PODDAR [1983, 3. ábra] 3-réteges modelljét használtuk, ahol $\sigma_1=0{,}01$ S/m, $\sigma_2=0{,}03$ S/m, $\sigma_3=0{,}001$ S/m, $h_1=3$ m, $f=1344$ Hz és h_2 úgy változott, ahogy azt a jelmagyarázat feltünteti
a) A H_z/Z_0 normált amplitúdó X függvényében,
b) a H_z/Z_0 fázis X függvényében,
c) a H_r/Z_0 normált amplitúdó X függvényében és
d) a H_r/Z_0 fázis X függvényében

Рис. 3. Дистанционное зондирование внутри контура ($a=b=250$ м), $Y=0$; X изменяется по 25 м от 25 м до 225 м. Использован трехслойный модель Поддара [1983, рис. 3], при котором $\sigma_1=0{,}01$ сименс/м, $\sigma_2=0{,}03$ сименс/м, $\sigma_3=0{,}001$ сименс/м, $h_1=3$ м, $f=1344$ Гц, h_2 изменяется согласно рисунку
а) нормированная амплитуда H_z/Z_0 в зависимости от X,
b) фаза H_z/Z_0 в зависимости от X,
c) нормированная амплитуда H_r/Z_0 в зависимости от X,
d) фаза H_r/Z_0 в зависимости от X

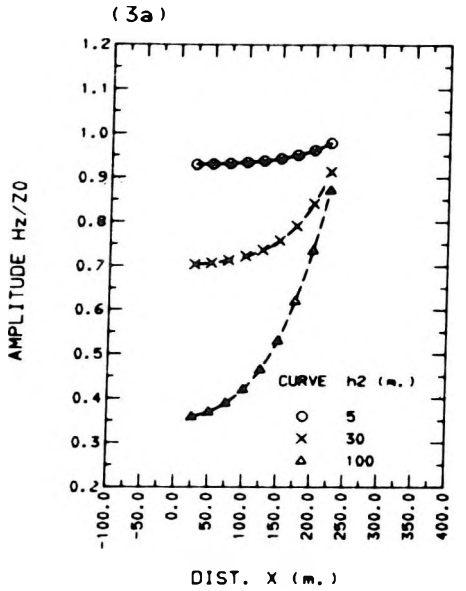
(3a)
AMPLITUDE Hz/Z0
DIST. X (m.)
CURVE h2 (m.)
5
30
100

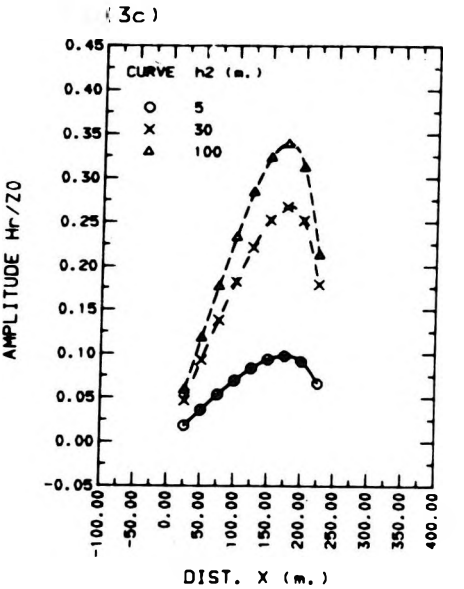
(3c)
AMPLITUDE Hr/Z0
DIST. X (m.)
CURVE h2 (m.)
5
30
100

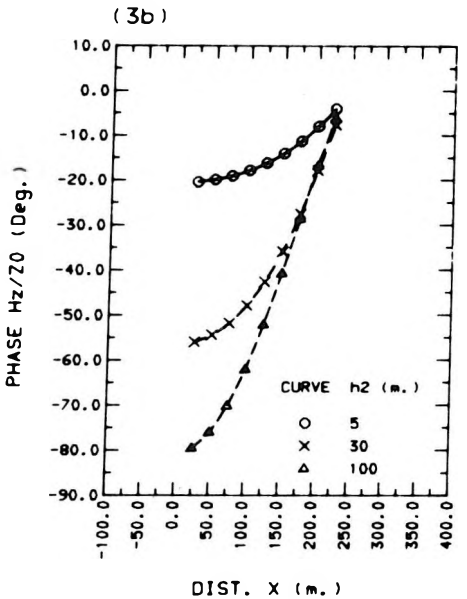
(3b)
PHASE Hz/Z0 (Deg.)
DIST. X (m.)
CURVE h2 (m.)
5
30
100

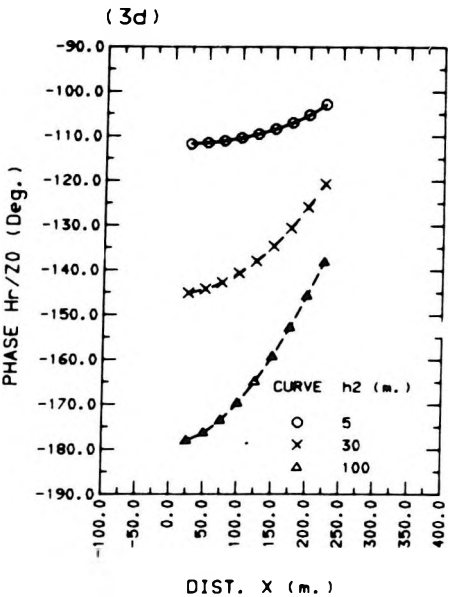
(3d)
PHASE Hr/Z0 (Deg.)
DIST. X (m.)
CURVE h2 (m.)
5
30
100

Fig. 4. Geometric soundings outside a square loop ($a=b=250$ m) at $Y=0$ where X was varied from 300 to 1000 m in increments of 100 m. The 3-layer model from PODDAR [1983, Fig. 3] was used, where $\sigma_1=0.01$ S/m, $\sigma_2=0.03$ S/m, $\sigma_3=0.001$ S/m, $h_1=3$ m, f=1344 Hertz, and h_2 was varied as indicated in the legends
a) Normalized amplitude H_z/Z_0 versus X,
b) phase H_z/Z_0 versus X,
c) normalized amplitude H_r/Z_0 versus X, and
d) phase H_r/Z_0 versus X

4. ábra. Geometriai szondázások a négyzet alakú hurkon ($a=b=250$ m) kívül $Y=0$-nál, X pedig 300 m-től 1000 m-ig változott 100 m-es lépésekben. PODDAR [983, 3. ábra] 3-réteges modelljét használtuk, ahol $\sigma_1=0{,}01$ S/m, $\sigma_2=0{,}03$ S/m, $\sigma_3=0{,}001$ S/m, $h_1=3$ m, $f=1344$ Hz és h_2 úgy változik, ahogy azt a jelmagyarázat feltünteti
a) A H_z/Z_0 normált amplitúdó X függvényében,
b) a H_z/Z_0 fázis X függvényében és
c) a H_r/Z_0 normált amplitúdó X függvényében
d) a H_r/Z_0 fázis X függvényében

Рис. 4. Дистанционные зондирования вне контура ($a=b=250$ м), $Y=0$; X изменяется по 100 м от 300 м до 1000 м. Использован трехслойный модель ПОДДАРА [1983, рис. 3], при котором $\sigma_1=0{,}01$ сименс/м, $\sigma_2=0{,}03$ сименс/м, $\sigma_3=0{,}001$ сименс/м, $h_1=3$ м, $f=1344$ Гц, h_2 изменяетсяпо по условным обозначениям
а) нормированная амплитуда H_z/Z_0 в зависимости от X,
b) фаза H_z/Z_0 в зависимости от X
c) нормированная амплитуда H_r/Z_0 в зависимости от X,
d) фаза H_r/Z_0 в зависимости от X

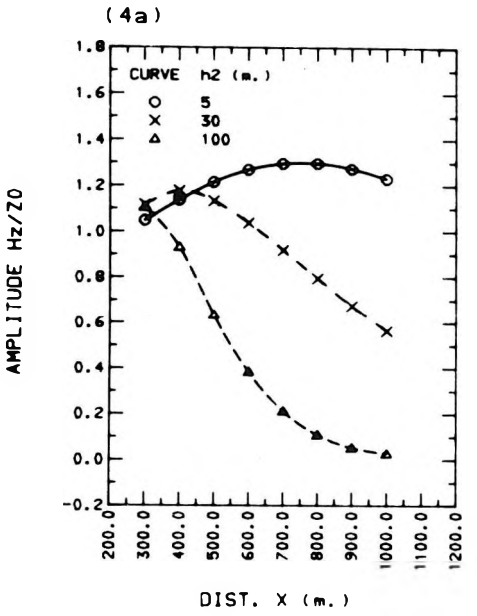
(4a)
CURVE h2 (m.)
5
30
100
AMPLITUDE Hz/Z0
DIST. X (m.)

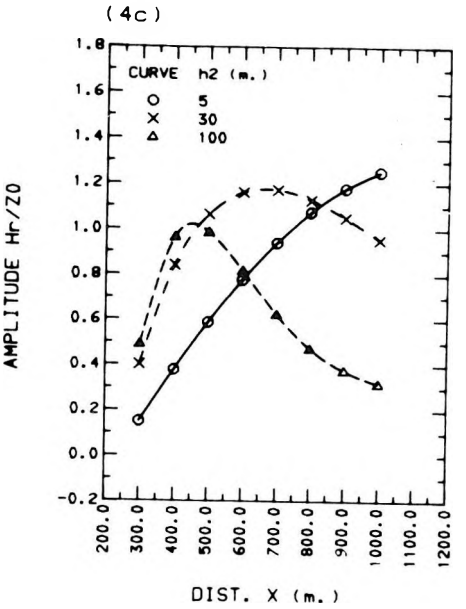
(4c)
CURVE h2 (m.)
5
30
100
AMPLITUDE Hr/Z0
DIST. X (m.)

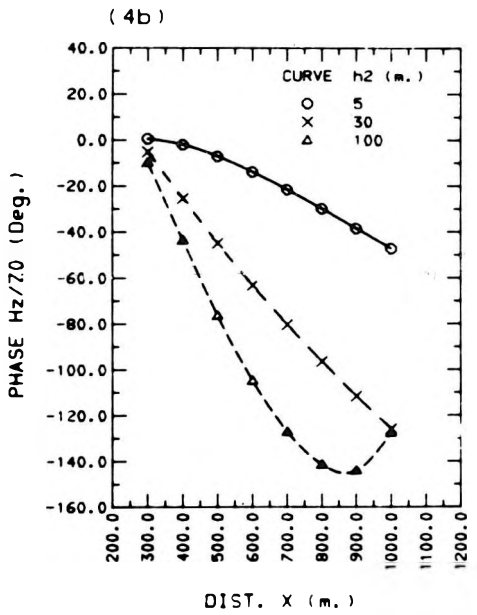
(4b)
CURVE h2 (m.)
5
30
100
PHASE Hz/Z0 (Deg.)
DIST. X (m.)

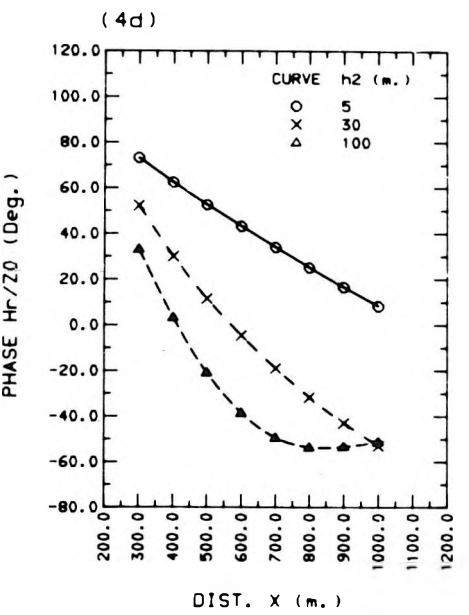
(4d)
CURVE h2 (m.)
5
30
100
PHASE Hr/Z0 (Deg.)
DIST. X (m.)

Fig. 5. Geometric soundings in quadrant I near the corner point (250,250) for a square loop ($a=b=250$ m) at $Y=275$ where X was varied from 0 to 500 m in increments of 50 m. The 3-layer model from PODDAR [1983, Fig. 3] was used, where $\sigma_1=0.01$ S/m, $\sigma_2=0.03$ S/m, $\sigma_3=0.001$ S/m, $h_1=3$ m, $f=1344$ Hertz, and h_2 was varied as indicated in the legends
a) Normalized amplitude H_z/Z_0 versus X,
b) phase H_z/Z_0 versus X,
c) normalized amplitude H_r/Z_0 versus X, and
d) phase H_r/Z_0 versus X

5. ábra. Geometriai szondázások az I. síknegyedben, a négyzet alakú hurok ($a=b=250$ m) (250,250) sarokpontjának közelében, $Y=275$-nél, X pedig 0-tól 500 m-ig változott 50 m-es lépésekben. PODDAR [1983, 3. ábra] 3-réteges modelljét használtuk, ahol $\sigma_1=0{,}01$ S/m, $\sigma_2=0{,}03$ S/m, $\sigma_3=0{,}001$ S/m, $h_1=3$ m, $f=1344$ Hz és h_2 úgy változott, ahogy azt a jelmagyarázat feltünteti
a) A H_z/Z_0 normált amplitúdó X függvényében,
b) a H_z/Z_0 fázis X függvényében,
c) a H_r/Z_0 normált amplitúdó X függvényében,
d) a H_r/Z_0 fázis X függvényében

Рис. 5. Дистанционные зондирования в первой четверти плоскости, вблизи угловой точки контура квадратной ($a=b=250$ м) формы. $Y=275$; X изменяется по 50 м от 0 до 500 м. Использован трехслойный модель ПОДДАРА [1983, рис. 3] при котором $\sigma_1=0{,}01$ сименс/м, $\sigma_2=0{,}03$ сименс/м, $\sigma_3=0{,}001$ сименс/м, $h_1=3$ м, $f=1344$ Гц, h_2 изменяется согласно условным обозначениям
а) нормированная амплитуда H_z/Z_0 в зависимости от X,
b) фаза H_z/Z_0 в зависимости от X,
c) нормированная амплитуда H_r/Z_0 в зависимости от X,
d) фаза H_r/Z_0 в зависимости от X

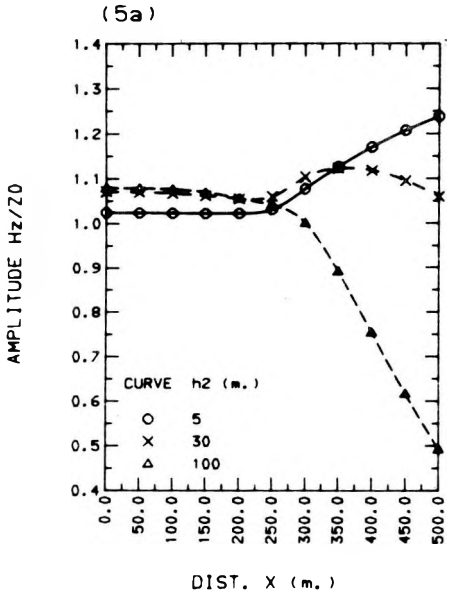
(5a)
AMPLITUDE Hz/Z0
CURVE h2 (m.)
5
30
100
DIST. X (m.)

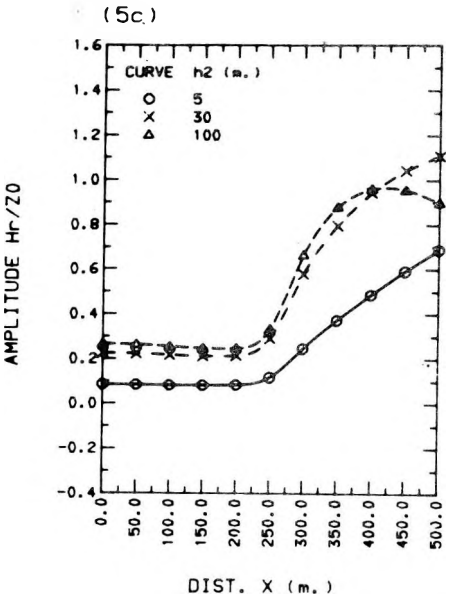
(5c)
AMPLITUDE Hr/Z0
CURVE h2 (m.)
5
30
100
DIST. X (m.)

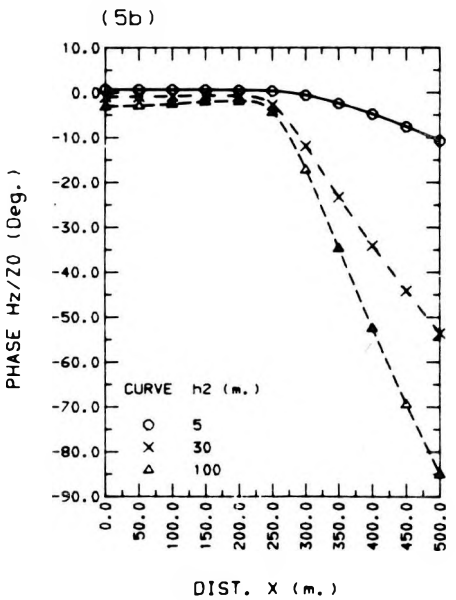
(5b)
PHASE Hz/Z0 (Deg.)
CURVE h2 (m.)
5
30
100
DIST. X (m.)

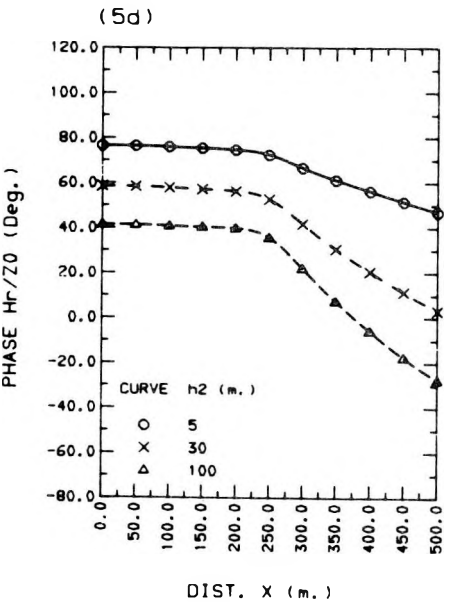
(5d)
PHASE Hr/Z0 (Deg.)
CURVE h2 (m.)
5
30
100
DIST. X (m.)

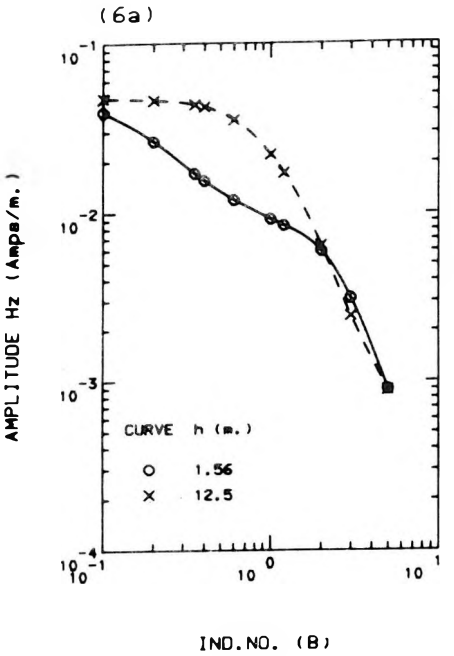
(6a)
AMPLITUDE Hz (Amps/m.)
CURVE h (m.)
1.56
12.5
IND.NO. (B)

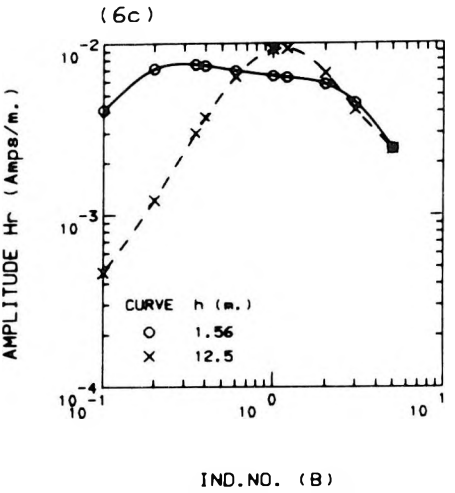
(6c)
AMPLITUDE Hr (Amps/m.)
CURVE h (m.)
1.56
12.5
IND.NO. (B)

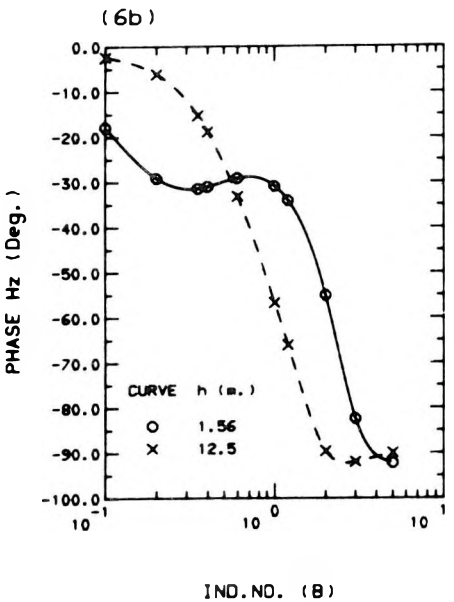
(6b)
PHASE Hz (Deg.)
CURVE h (m.)
1.56
12.5
IND.NO. (B)

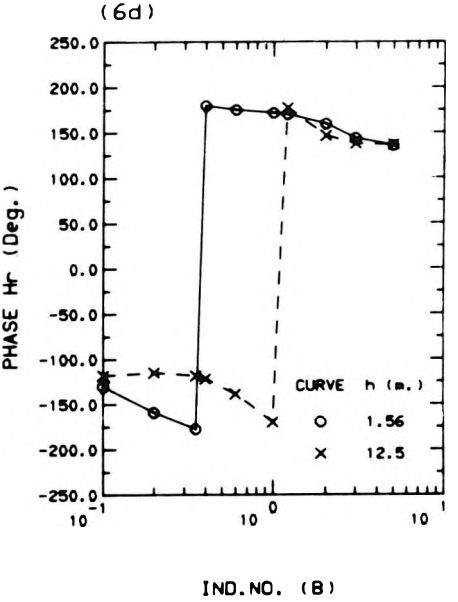
(6d)
PHASE Hr (Deg.)
CURVE h (m.)
1.56
12.5
IND.NO. (B)

Fig. 6. Parametric soundings near the loop center for a square loop ($a = b = 10$ m) at the point ($X = 2$, $Y = 3$), and computed over a given induction number ($B = R_0/\delta$) range. The 2-layer model from PODDAR [1983, Fig. 2] was used, where $\sigma_1 = 0.01$ S/m, $\sigma_2 = 0.3$ S/m, and h was varied as indicated in the legends
a) Unnormalized amplitude H_z versus B,
b) phase H_z versus B,
c) unnormalized amplitude H_r versus B, and
d) phase H_r versus B.

6. ábra. Paraméter szondázások egy négyzet alakú hurok ($a = b = 10$ m) középpontjának közelében, az ($X = 2$, $Y = 3$) pontban, egy adott indukció szám ($B = R_0/\delta$) tartományon számítva. PODDAR [1983, 2. ábra] 2-réteges modelljét használtuk, ahol $\sigma_1 = 0{,}01$ S/m, $\sigma_2 = 0{,}3$ S/m és h úgy változott, ahogy a jelmagyarázat feltünteti
a) A normálatlan H_z amplitúdó B függvényében,
b) a H_z fázis B függvényében,
c) a normálatlan H_r amplitúdó B függvényében és
d) a H_r fázis B függvényében

Рис. 6. Параметрические зондирования вблизи центра контура квадратной формы, ($a = b = 10$ м), в точке ($X = 2$, $Y = 3$), для данного интервала чисел индукции ($B = R_0/\delta$). Использован двухслойный модель ПОДДАРА [1983, рис. 2], при котором $\sigma_1 = 0{,}01$ сименс/м, $\sigma_2 = 0{,}3$ сименс/м, h изменяется согласно условным обозначениям
a) ненормированная амплитуда H_z в зависимости от B,
b) фаза H_z в зависимости от B,
c) ненормированная амплитуда H_r в зависимости от B,
d) фаза H_r в зависимости от B

5. Conclusions

A new algorithm was discussed that evaluates simultaneously the radial H_r and vertical H_z magnetic fields inside or outside a rectangular loop source of current on a multilayered earth. A fast Hankel transform algorithm [ANDERSON 1982] is the basis for the new solution, which in turn, reduces the overall computation of either H_r or H_z to four elementary spline-function integrations. Accuracy of this method is at least comparable to that obtained with dipole or circular loop source methods. Because of the improved speed of the calculations, future uses of this technique during inverse solutions in either frequency- or time-domains would be nearly as practical for rectangular loops as for dipole sources. The general idea presented can be readily extended to additionally compute the electric field components about a rectangular loop source. Further extensions and savings could be realized by storing intermediate FHT results for repetitive calculations using the same earth model while varying the loop size and/or position.

REFERENCES

ALBERG J. H., NILSON E. N., and WALSH J. L. 1967: The theory of splines and their applications. Academic Press, New York, 284 p.

ANDERSON W. L. 1979: Numerical integration of related Hankel transforms of orders 0 and 1 by adaptive digital filtering. Geophysics, **44,** 7, pp. 1287–1305

ANDERSON W. L. 1982: Fast Hankel transforms using related and lagged convolutions. Association for Computing Machinery Transactions on Mathematical Software, **8,** 4, pp. 344–368

ANDERSON W. L. 1984: Fast evaluation of Hr and Hz field soundings near a rectangular loop source on a layered earth (Program HRZRECT). U.S. Geological Survey Open-File Report 84–257, 80 p.

ANDERSON W. L. 1985: Computation of transient soundings for the time-derivative of Hz near a rectangular loop source on a layered earth (Program FWDTHZ). U.S. Geological Survey Open-File Report 85–270, 44 p.

BOERNER D. E., and WEST G. F. 1984: Efficient calculation of the electromagnetic fields of an extended source. Geophysics, **49,** 11, pp. 2057–2060

FRISCHKNECHT F. C. 1967: Fields about an oscillating magnetic dipole over a two-layer earth and application to ground and electromagnetic surveys. Quarterly of the Colorado School of Mines, **62,** 1, 326 p.

KAUAHIKAUA J. 1978: Electromagnetic fields about a horizontal electric wire source of arbitrary length. Geophysics, **43,** 5, pp. 1019–1022

KRISTENSSON G. 1983: The electromagnetic field in a layered earth induced by an arbitrary stationary current distribution. Radio Science, **18,** 3, pp. 357–368

PATTERSON T. N. L. 1973: Algorithm for automatic numerical integration over a finite interval. Comm. of the ACM, **16,** 11, pp. 694–699

PODDAR M. 1982: A rectangular loop source of current on a two-layered earth. Geophysical Prospecting, **30,** 1, pp. 101–114

PODDAR M. 1983: A rectangular loop source of current on multilayered earth. Geophysics, **48,** 1, pp. 107–109

RYU J., MORRISON H. F., and WARD S. H. 1970: Electromagnetic fields about a loop source of current. Geophysics, **35,** 5, pp. 862–896

WAIT J. R. 1958: Induction by an oscillating dipole over a two-layer ground. Appl. Sci. Res., v. B–7, pp. 73–80

WAIT J. R. 1966: Fields of a horizontal dipole over a stratified anisotropic half-space. IEEE Trans. on Antennas and Propagation, **AP–14,** 6, pp. 790–792

A RADIÁLIS ÉS FÜGGŐLEGES MÁGNESES TÉR GYORS SZÁMÍTÁSA RÉTEGZETT FÖLDÖN FEKVŐ, TÉGLALAP ALAKÚ HUROKFORRÁS KÖZELÉBEN

Walter L. ANDERSON

Gyors Hankel-transzformációs (FHT) algoritmust alkalmaz a rétegzett föld felszínén fekvő, téglalap alakú hurokforráson belüli vagy azon kívüli, radiális vagy függőleges mágneses tér felhasználásával végzett paraméter (vagy geometriai) szondázások görbéinek egyidejű számítására. Az FHT a lineáris digitális szűrés elvét használja fel és ha a téglalap alakú hurok problémájára alkalmazzuk, minden egyes térszámítás négy elemi spline integrálásra egyszerűsödik. Paraméter szondázás esetén az FHT-re csak egyszer van szükség minden egyes frekvencián; geometriai szondázás esetén az FHT-t csak egyszer kell végrehajtani ahhoz, hogy megkapjuk mindkét térösszetevőt. Az FHT módszernek a meglévő, dipólra, köralakú és téglalap alakú hurokra vonatkozó egyenes feladat megoldásokkal való összehasonlítása azt mutatja, hogy legalább három számjegyes pontosság érhető el jelentősen csökkentett számítási idő mellett is. Ennek következtében az inverz feladat megoldása mind a frekvencia-, mind az időtartományban gyakorlatilag is lehetséges lesz téglalap alakú hurokforrása éppúgy, mint dipólforrásra.

БЫСТРОЕ ВЫЧИСЛЕНИЕ РАДИАЛЬНОГО И ВЕРТИКАЛЬНОГО МАГНИТНОГО ПОЛЯ ВБЛИЗИ ВОЗБУЖДАЮЩЕЙ ПЕТЛИ ПРЯМОУГОЛНОЙ ФОРМЫ, НАХОДЯЩЕЙСЯ НА ПОВЕРХНОСТИ СЛОИСТОЙ СРЕДЫ

Вальтер Л. АНДЕРСОН

Применяется алгоритм быстрой Хенкел-трансформации (FHT) для вычисления кривых зондирований (параметрических или дистанционных), проведенных с применением радиальных или вертикальных компонентов магнитного поля прямоугольного контура, находящегося на поверхности слоистой среды. При FHT используется принцип линейной цифровой фильтрации. В случае прямоугольного контура вычисления полей превращается в интеграцию четырех элементарных «сплайнов». При параметрическом зондировании нужен FHT только раз на каждую частоту. При геометрическом зондировании для вычисления обоих компонентов нужен FHT только один раз. Сопоставление результатов, полученных с применением FHT с результатами существующих решений прямых задач для диполя и петлей круглой и прямоугольной форм указывает на то, что достигается точность порядка трех цифров, существенно сокращая и время вычислений. Благодаря этого практически можно решать и обратные задачи для прямоугольного контура и для диполя так в частотных, как и временных диапазонах.